Biosensors and Bioelectronics 145 (2019) 111700

Contents lists available at ScienceDirect

Biosensors and Bioelectronics

journal homepage: www.elsevier.com/locate/bios

# Terminal deoxynucleotidyl transferase-activated nicking enzyme amplification reaction for specific and sensitive detection of DNA methyltransferase and polynucleotide kinase

Yi-Chen Du, Si-Yuan Wang, Xiao-Yu Li, Ya-Xin Wang, An-Na Tang, De-Ming Kong*

*State Key Laboratory of Medicinal Chemical Biology, Tianjin Key Laboratory of Biosensing and Molecular Recognition, Research Centre for Analytical Sciences, College of Chemistry, Nankai University, Tianjin, 300071, PR China*

ARTICLE INFO

*Keywords:*
DNA methyltransferase
Polynucleotide kinase
Terminal deoxynucleotidyl transferase
Nicking enzyme amplification reaction
Fluorescence

ABSTRACT

DNA methyltransferase (MTase) and polynucleotide kinase (PNK) are both DNA-dependent enzymes that play important roles in DNA methylation and DNA repair processes, respectively. Dysregulation of their activities is associated with various human diseases. Herein, we present a specific and sensitive biosensing strategy, named terminal deoxynucleotidyl transferase (TdT)-activated nicking enzyme amplification reaction (TdT-NEAR), for their activity detection. As for MTase detection, an enclosed dumbbell-shaped oligonucleotide substrate, whose symmetric stem containing a recognition site of Dam MTase and an incomplete recognition sequence of nicking endonuclease Nt.BbvCI, was used. Typically, the substrate is methylated by Dam MTase and subsequently cleaved by Dpn I. In the presence of TdT and dGTP, poly(guanine, G) sequences are extended from the released 3′-OH ends, achieving the conversion of the incomplete Nt.BbvCI recognition sequence to an intact one. The extension products can then be used to trigger Nt.BbvCI-catalyzed cyclic cleavage of fluorophore/quencher-labelled oligonucleotide probe, giving a significantly enhanced fluorescence output. Such a sensing system can achieve sensitive and specific detection of Dam MTase with a detection limit of 0.002 U/mL. The unique working mechanism endows the sensing system with improved anti-interference capability and thus increased application potential in complex biological samples. Moreover, it was also demonstrated to work well for Dam MTase inhibitor screening and inhibitory activity evaluation, thus holding great potential in disease diagnosis and drug discovery. Using a simpler 3′-phosphorylated linear substrate and the same fluorescent probe, the TdT-NEAR strategy can be easily extended to the activity analysis of PNK, thus revealing wide application potential in bioanalysis.

## 1. Introduction

DNA methyltransferase (MTase) and polynucleotide kinase (PNK) are both DNA-dependent enzymes, and both play crucial roles in physiological process and disease development. MTase is a key participator in DNA methylation, an important epigenetic modification that plays significant roles in gene expression, genomic stability, cell growth and development (Reik et al., 2001). During methylation process, MTase can transfer a methyl group from S-adenosylmethionine (SAM) to cytosine or adenine bases in DNA (Cheng and Roberts, 2001; Smith and Meissner, 2013). Recent researches demonstrate that abnormal MTase activity causes improper regulation of methylation, inactivates the tumor suppressor genes and thus is closely associated with initiation and progression of various types of cancer (Rajendran et al., 2011; Robertson et al., 1999; Roll et al., 2008; Shukl et al., 2010). Therefore, MTase has become a promising biomarker and a potential therapeutic target for cancer. As an important DNA repair enzyme, PNK is able to catalyze not only the phosphorylation of nucleic acids with 5′-OH ends, but also the dephosphorylation of nucleic acids with 3′-phosphate ends, and thus plays crucial roles in DNA repair (Lindahl and Wood, 1999). Abnormal activity of PNK has been reported to disturb the DNA lesion repair process, and thus resulting in variety of human diseases (Sharma et al., 2006). Therefore, development of highly sensitive and specific sensing platform for MTase and PNK activity analysis is of significance for both drug discovery and fundamental biochemical research.

Conventional methods for MTase and PNK activity detection include high-performance liquid chromatography (HPLC) (Wenzel and Guschlbauer, 1993), gel electrophoresis (Bernstein et al., 2005; Rebeck and Samson, 1991), radioactive assay (Chappell et al., 2002; Kim et al., 2004) and immunochemical approaches (Boye et al., 1992). However,

* Corresponding author.
*E-mail address:* kongdem@nankai.edu.cn (D.-M. Kong).

https://doi.org/10.1016/j.bios.2019.111700
Received 24 July 2019; Received in revised form 28 August 2019; Accepted 11 September 2019
Available online 12 September 2019
0956-5663/ 

hazardous radiation, low sensitivity, sophisticated instruments and complicated manipulation limit the practical applications of these techniques. Alternatively, some new approaches such as colorimetry (Jiang et al., 2014; Wu et al., 2013), electrochemistry (Chen et al., 2019b; Cui et al., 2018a, 2018b; Hou et al., 2019; Ji et al., 2016; Peng et al., 2013; Wang et al., 2013), chemiluminescence (He et al., 2014; Zeng et al., 2013), fluorescence (Hou et al., 2014; Li et al., 2007, 2018a; Lin et al., 2011; Wang et al., 2017) and nanopore-based assay (Rauf et al., 2017) have been developed. To improve the detection sensitivity, various signal amplification strategies have been introduced, including exonuclease aided target recycling (Lin et al., 2011; Xing et al., 2014), duplex-specific nuclease-assisted amplification (Zhang et al., 2015), rolling circle amplification (Chen et al., 2019a; Huang et al., 2017; Jiang et al., 2014; Li et al., 2017) and strand displacement amplification (Cheng et al., 2015; Cui et al., 2019; Wang et al., 2018). In these methods, template-dependent DNA polymerization reactions are often required. Therefore, most of them involve complicated design of DNA probes and inevitably suffer from high backgrounds due to nonspecific hybridization of templates. Thus, a simple method with high sensitivity and good specificity is highly desirable.

In this research, we develop a simple and specific sensing strategy, named as terminal deoxynucleotidyl transferase (TdT)-activated nicking enzyme amplification reaction (TdT-NEAR), for the sensitive detection of DNA MTase and PNK activity. TdT is a template-independent DNA polymerase that catalyzes the repetitive addition of deoxyribonucleotides to the 3′-hydroxyl (3′-OH) end of a DNA or RNA strand (Faber et al., 2000; Yuan et al., 2014). Due to the unique property, TdT has currently been exploited as a powerful tool for bioanalysis (Deng et al., 2019; Du et al., 2018a, 2018b; Liu et al., 2014; Zhou et al., 2019). Nt.BbvCI is a nicking endonuclease that can cut one strand in a DNA duplex at a specific recognition site. Taking advantage of Nt.BbvCI-catalyzed cyclic signal amplification, the proposed strategy showed high sensitivity for DNA MTase and PNK activity detection. What's more, our sensing platform also demonstrated to work well for screening their inhibitors and quantifying their activities in complex biological samples (including human serum and cancer cells), thus holding great potential in biomedical research and clinical diagnosis.

## 2. Experimental section

### 2.1. Materials and reagents

The oligonucleotides used in this work (Table 1) were synthesized and purified by Sangon Biotech. Co. Ltd. (Shanghai, China). Methyltransferase of DNA adenine methylation (Dam MTase), methyltransferase of DNA cytosine methylation (M.SssI MTase), Dpn I endonuclease, S-adenosylmethionine (SAM), terminal deoxynucleotidyl transferase (TdT), nicking endonuclease Nt.BbvCI, T4 polynucleotide kinase (PNK), T4 DNA ligase, exonuclease I (Exo I), exonuclease III (Exo III) and corresponding buffer solutions were obtained from New England Biolabs (Beijing, China). 5-Fluorouracil and healthy human serum were bought from Solarbio (Beijing, China). All chemical reagents were of analytical grade and used without further purification.

### 2.2. Preparation of enclosed dumbbell-shaped Dam MTase substrate

47 μL reaction mixture containing 5 μL of $\mathbf{S_{Dam}}$ solution (100 μM) and 5 μL 10 × T4 DNA ligase buffer was incubated at 95 °C for 5 min, and then cooled down to 25 °C to ensure the formation of dumbbell-shaped structure. Next, 400 U of T4 DNA ligase was added into the mixture and the ligation reaction was conducted at 16 °C for 12 h. After that, 1 μL of Exo I (20 U/μL) and 1 μL of Exo III (100 U/μL) were added to a final volume of 50 μL, and the mixture was incubated at 37 °C for 1 h to completely digest the leftover unreacted substrates. The enzymes were then inactivated by heating the mixture at 80 °C for 20 min. The obtained solution containing enclosed dumbbell-shaped substrate ($\mathbf{eS_{Dam}}$) could be directly used in the following experiments or was stored at −20 °C for further use.

### 2.3. Detection of Dam MTase activity

First, 4 μL as-prepared $\mathbf{eS_{Dam}}$ solution was added into a solution (25 μL) containing different concentrations of Dam MTase, 160 μM SAM, 6 U of Dpn I, 2.5 μL of 10 × Dam MTase reaction buffer and 2.5 μL of 10 × CutSmart buffer. The solution was incubated at 37 °C for 45 min. Second, 10 μL of above reaction solution was added into 30 μL of reaction system containing 2 μL of dGTP (100 mM), 3 μL of 10 × TdT buffer, 3 μL of $CoCl_2$ (2.5 mM) and 15 U of TdT, followed by incubation at 37 °C for 60 min. After that, TdT polymerase was inactivated by heating the solution at 80 °C for 10 min. Next, 7 μL of 10 × CutSmart buffer, 3 μL of **F-Q** probe (10 μM), 10 U of Nt.BbvCI were added in. The mixture with a total volume of 100 μL was incubated for 1 h at 37 °C. End-point fluorescence spectra were measured on a Shimadzu RF-5301 fluorescence spectrometer (Shimadzu Ltd., Japan) using 492 nm as the excitation wavelength. The fluorescence intensity at 517 nm was collected for quantitative assay of Dam MTase activity. For real-time monitoring of fluorescence, 30 μL of above reaction mixture was incubated at 37 °C on the ABI StepOne Plus real-time PCR system (Applied Biosystems), and the fluorescence was automatically recorded at an interval of 1 min.

### 2.4. Inhibition assay of Dam MTase activity

For Dam MTase activity inhibition assay, different amounts of 5-fluorouracil were preincubated with $\mathbf{eS_{Dam}}$ at 37 °C for 15 min before addition of 0.4 U/mL Dam MTase (final concentration). The Dam MTase activity was measured as described above, and its relative activity (RA) was calculated based on eqn: $RA = (F_i - F_0)/(F_t - F_0)$, where $F_0$, $F_t$, and $F_i$ represent the fluorescence intensity in the absence of Dam MTase, in the presence of 0.4 U/mL Dam MTase, and in the presence of 0.4 U/mL Dam MTase and different concentrations of 5-fluorouracil, respectively.

### 2.5. Dam MTase recovery assay from human serum sample

Dam MTase recovery analysis was performed under similar experimental conditions to those used for Dam MTase activity assay, excepting addition of 5% human serum sample in the methylation step.

**Table 1**
The oligonucleotides used in this work.

| Oligonucleotide | Sequence (5′→3′) |
|---|---|
| $\mathbf{S_{Dam}}$ | P-*TCAGC* TTAGT ACATT *GCTGA* TCAGC CATGA TGATT GCTGA |
| **MP** | *TCAGC* TTAGT ACATT *GCTGA* **GGGGG GGGGG** |
| **F-Q** | FAM- CCCCC TCAGC AAT -BHQ1 |
| Random oligonucleotide | CGTGC AGCTC GTTAC CACCA CCACC ACAAC CACCA CCACC GATCT AACCT ATCCG ATCGA GCTGC ACG |
| $\mathbf{S_{PNK}}$ | TTAGT ACATT GCTGA-P |

Italic regions in $\mathbf{S_{Dam}}$ and **MP** are complementary. Underlined regions in $\mathbf{S_{Dam}}$ are complementary. 'P' indicates phosphate group. 'FAM' indicates 6-carboxyfluorescein. 'BHQ1' indicates black hole quencher 1 modification.

The Dam MTase activity was measured using the same procedures as those described above.

### 2.6. Polyacrylamide gel electrophoresis (PAGE) analysis

The reaction products were analyzed by 10% PAGE in 1 × TAE buffer (40 mM Tris, 20 mM acetic acid, 1 mM EDTA, pH 8.3) at a 120 V constant voltage for 50 min. The gel was stained with 2 × Gel Red and photographed using a Gel Documentation system (Huifuxingye, Beijing, China).

### 2.7. T4 PNK activity assay

The assay was carried out in 40 μL of reaction solution containing 0.4 μM of **$S_{PNK}$**, different concentrations of T4 PNK, 2 μL of 10 × PNK reaction buffer, 2 μL of 10 × TdT buffer, 2 μL of dGTP (100 mM) and 15 U of TdT. The samples were incubated at 37 °C for 60 min to perform the 3′-dephosphorylation of **$S_{PNK}$** and TdT polymerization reaction. After that, TdT polymerase was inactivated by heating the solution at 80 °C for 10 min. Next, 6 μL of 10 × CutSmart buffer, 3 μL of **F-Q** probe (10 μM), 10 U of Nt.BbvCI were added in. The mixture with a total volume of 100 μL was incubated for 1 h at 37 °C. Fluorescence spectra were measured using 492 nm as the excitation wavelength. The fluorescence intensity at 517 nm was collected for the quantitative assay of PNK activity. For PNK inhibition assay, $(NH_4)_2SO_4$ was used as the model inhibitor. Various concentration of inhibitors were mixed with **$S_{PNK}$** and incubated for 15 min prior to the dephosphorylation and polymerization reactions.

### 2.8. PNK activity analysis in cell lysates

HeLa (human cervical cancer cell line) cells were grown in Dulbecco's modified Eagle's medium (DMEM), supplemented with penicillin (100 U/mL), streptomycin (100 μg/mL) and 10% fetal bovine serum and incubated at 37 °C in a humidified atmosphere of 5% $CO_2$ and 95% air. The cell lysates were prepared using a nucleoprotein extraction kit (Sangon Biotech, Shanghai, China) according to the manufacturer's protocol. The collected cell lysates were used for PNK activity assay immediately or stored at −80 °C until use. The detection procedures were same as those described above but cell lysates were added in the sensing systems instead of T4 PNK.

## 3. Results and discussion

### 3.1. Design of TdT-NEAR strategy for Dam MTase activity detection

First, the feasibility of the proposed signal amplification strategy for MTase activity analysis was tested. Dam MTase was selected as the model DNA MTase, it can catalyze the transfer of a methyl group from SAM to the N6 position of adenine residue in the palindromic sequence of 5′-GATC-3'. Accordingly, we designed an enclosed dumbbell-shaped substrate (called **$eS_{Dam}$**), whose symmetric stem 5′-GCTGATCAGC-3′ contains a recognition sequence of Dam MTase and an incomplete recognition sequence (5′-GCTGA-3′) of Nt.BbvCI. This substrate was prepared by self-template ligation of a 5′-phosphorylated DNA oligonucleotide **$S_{Dam}$** (Table 1 and Fig. S1) (Huang et al., 2017). The working mechanism of TdT-NEAR strategy for Dam MTase activity assay is illustrated in Scheme 1. In the presence of Dam MTase and SAM, the 5′-GATC-3′ sequences in double-stranded stem of **$eS_{Dam}$** would be methylated at the adenine bases. The methylated **$eS_{Dam}$** was subsequently cleaved by endonuclease Dpn I, releasing two hairpin-like fragments, each of which contains a free 3′-OH termini. Then, TdT-catalyzed polymerization reaction can be started at the 3′-OH ends using dGTP as the "fuel". With the addition of poly(guanine, G) sequence at the 3′-end, the incomplete Nt.BbvCI recognition sequence converts to an intact one (5′-GCTGAGG-3′). Then, the hairpin structure of the extended product

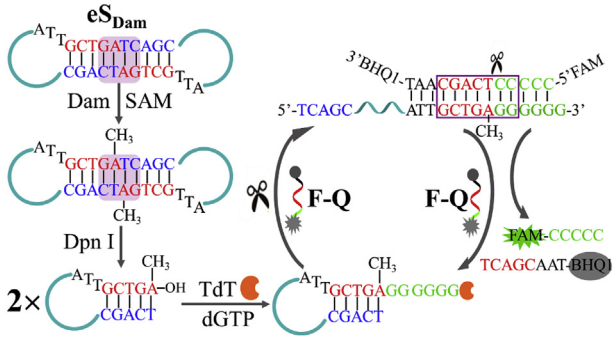


**Scheme 1.** Schematic illustration of TdT-NEAR-based Dam MTase activity assay.

is opened and hybridizes with a fluorophore/quencher-labelled reporter probe (named **F-Q**, Table 1). Due to the presence of intact Nt.BbvCI recognition sequence, the hybridized **F-Q** probe is specifically cleaved into two parts and then released from the DNA duplex, resulting in the complete separation of the fluorophore (FAM) and the quencher (BHQ1), accompanied by the recovery of the previously quenched fluorescence. The released hairpin sequence will then bind with another **F-Q** probe and trigger the "hybridization-cleavage-releasing" cycles, enabling fluorescence signal to be greatly amplified. In the absence of Dam MTase, however, the dumbbell-shaped **$eS_{Dam}$** keeps intact, and neither TdT-mediated DNA extension nor Nt.BbvCI-catalyzed **F-Q** cleavage can be initiated. As a result, fluorescence change is barely observed.

To demonstrate the proposed mechanism, nondenaturating polyacrylamide gel electrophoresis (PAGE) was first performed to verify the Dam MTase/Dpn I-triggered methylation/cleavage reaction of **$eS_{Dam}$** and subsequent TdT-catalyzed extension of cleavage products. As shown in Fig. 1a, in the presence of Dam MTase and Dpn I, a new DNA band (Lane 2) with faster migration rate than intact **$eS_{Dam}$** (Lane 1) appeared, suggesting the successful initiation of **$eS_{Dam}$** methylation and cleavage event. With the further addition of TdT, poly(G) sequence could be extended from the 3′-OH ends of the released cleavage products, and a new band was given (Lane 3). Since this new band showed a comparable migration rate to a mimic extension product **MP** (Table 1) with a $G_{10}$ sequence at the 3′-end (Fig. S2), it can be suggested about 10 G nucleotides were extended from the released cleavage products.

After demonstrating that **$eS_{Dam}$** could be cleaved by Dam MTase/Dpn I and then be extended by TdT, we next verify that the extension product could be used as the substrate to trigger the cleavage reaction of **F-Q** probe. Due to containing the complimentary sequence to **F-Q** probe and intact Nt.BbvCI recognition site, **MP** could be used as the substrate to trigger the cleavage of **F-Q** probe, which was reflected by the significant increase of fluorescence signal (Fig. 1b). Interestingly, in the presence of identical concentration of **F-Q**, the fluorescence signals of the two systems with different **MP** to **F-Q** ratios (1:1 or 0.1:1) could reach a similar level, although different reaction time was needed. This result implies that **MP** can be repeatedly used to trigger the cleavage of multiple **F-Q** strands. On the contrary, almost no detectable fluorescence change was observed when dumbbell-shaped **$eS_{Dam}$** was used to substitute **MP**, indicating that Dam MTase-initiated conversion of **$eS_{Dam}$** to TdT-catalyzed extension product is indispensable for fluorescence enhancement.

Having demonstrated the feasibility of each step in the proposed working mechanism, it is reasonably to believe that our sensing strategy can be used for Dam MTase activity detection. As expected, significantly enhanced fluorescence response was given by the sensing system towards Dam MTase (Fig. 1c), while none of the negative controls lacking Dam MTase, **$eS_{Dam}$**, Dpn I, TdT, dGTP or Nt.BbvCI exhibited observable fluorescence signal changes.

TdT is a sequence-independent nucleic acid polymerase, it can work

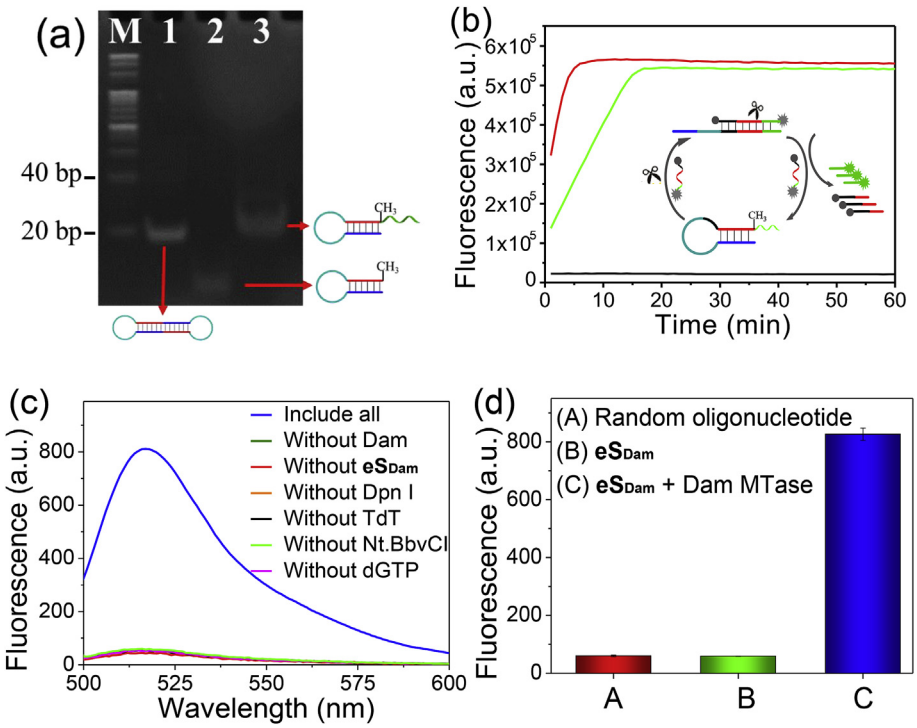


**Fig. 1.** (a) Nondenaturing PAGE analysis of Dam MTase/Dpn I-triggered methylation/cleavage reaction and TdT-catalyzed extension of cleavage products. Lane M is the DNA ladder marker. Lane 1: **eS$_{Dam}$**; Lane 2: **eS$_{Dam}$** + Dam MTase + Dpn I; Lane 3: **eS$_{Dam}$** + Dam MTase + Dpn I + TdT. (b) Time-dependent fluorescence change of Nt.BbvCI-catalyzed **F-Q** cleavage using **MP** as the substrate. Red line: **MP** (300 nM) + **F-Q** + Nt.BbvCI; Green line: **MP** (30 nM) + **F-Q** + Nt.BbvCI; Black line: **eS$_{Dam}$** (300 nM) + **F-Q** + Nt.BbvCI. [**F-Q**] = 300 nM, [Nt.BbvCI] = 100 U/mL. (c) Fluorescence assay for different sensing systems. [Dam MTase] = 8 U/mL. (d) Fluorescence signals given by the sensing systems containing **eS$_{Dam}$** or a random oligonucleotide. Error bars show the standard deviation of three independent experiments. (For interpretation of the references to color in this figure legend, the reader is referred to the Web version of this article.)

on any DNA or RNA substrates with 3′-OH termini. Such a characteristic is a double-edged sword. On one hand, it has been elegantly used in the design of biosensors. On the other hand, it increases the difficulty of the biosensor applications in real biological samples. In most reported TdT-based sensing systems, magnetic separation (Zhu et al., 2018) or/and 3′-end modification of oligonucleotides (Zhang et al., 2017) is usually adopted to prevent TdT-catalyzed undesirable extension of non-target oligonucleotides in the systems. However, high background level might also be given due to the destruction of the 3′-modification by enzymes or the presence of irrelevant DNAs or RNAs in biological samples. In our MTase-sensing system, when a random oligonucleotide (Table 1) with 3′-OH termini was added instead of **eS$_{Dam}$**, TdT-catalyzed oligonucleotide extension could also be observed (Fig. S3), but almost no detectable fluorescence increase compared to the blank control was given (Fig. 1d). This result indicates that the observed fluorescence increase is related with not only TdT-catalyzed oligonucleotide extension, but also the formation of intact Nt.BbvCI recognition site. Such a working mechanism will certainly increase the anti-interference capability of the biosensor, thus increase the possibility of its application in real biological samples.

### 3.2. Sensitivity of Dam MTase assay

Above experiments clearly demonstrate that the proposed sensing strategy can be applied for the detection of Dam MTase activity. To achieve the best performance, the experimental conditions, including amounts of **eS$_{Dam}$**, Dpn I, TdT and time for methylation/cleavage and TdT-catalyzed extension reactions, were optimized (Fig. S4 ~ Fig. S8). Under the optimized conditions (0.4 μM of **eS$_{Dam}$**, 6 U of Dpn I, 15 U of TdT, 45 min for methylation/cleavage reaction and 1 h for TdT-catalyzed extension reaction), the sensitivity of the Dam MTase-sensing system was evaluated by recording the fluorescence signal change as a function of Dam MTase concentration (Fig. 2a). As the Dam MTase concentration increased, a growing number of **eS$_{Dam}$** strands were cleaved for subsequent TdT-catalyzed extension reaction to form extension products containing intact Nt.BbvCI recognition sequence. Then, more and more reporter probes could be cleaved, thus giving Dam MTase concentration-dependent fluorescence increase. Fig. 2b shows the variance of fluorescence intensity at 517 nm with the concentration of Dam MTase. The fluorescence intensity exhibits a linear correlation with the Dam MTase concentration over a range from 0.01 to 4 U/mL (Fig. 2b). The linear regression equation is $F = 67.52 + 139.80C$ with a correlation coefficient ($R^2$) of 0.9928, where $F$ represents the fluorescence intensity and $C$ is the Dam MTase concentration. By evaluating the average response of blank controls plus three times the standard deviation, the detection limit was calculated to be 0.002 U/mL, which is better than or comparable to those of the reported methods (Table S1) (Ma et al., 2017; Rauf et al., 2017; Xu et al., 2018; Zhang et al., 2017). The high sensitivity was attributed to the excellent signal amplification efficiency of Nt.BbvCI-catalyzed **F-Q** cleavage.

To further simplify the experimental operations, we also tried to conduct Dam MTase activity assay by using a real-time fluorescence-monitoring mode. In such a mode, fluorescence change of the sensing system was synchronously recorded during Nt.BbvCI-catalyzed signal amplification process via a commercial real-time quantitative PCR instrument. As expected, $\Delta F \sim$ time curves (where $\Delta F$ is the fluorescence signal change compared to the initial value) showing distinct Dam MTase concentration-dependent fluorescence increasing rates were obtained (Fig. 2c). Using the derived $\lg(\Delta F) \sim$ time curves (Fig. 2d), the $RT_t$ values (the reaction time at which $\lg(\Delta F)$ reaches the set threshold) could extracted, and a linear relationship between $RT_t$ value and the logarithm of Dam MTase concentration was obtained in the range of 0.01–8 U/mL (Fig. 2e). Thanks to the unique data-processing method, the sensing system containing 0.01 U/mL Dam MTase could be discriminated from the blank control much more clearly in real-time mode than in end-point one. In addition, compared to end-point detection, such a real-time detection mode is simpler, more rapid and automatic due to the elimination of signal detection step after amplification, and thus more suitable for high-throughput detection of samples.

### 3.3. Selectivity of Dam MTase assay

To evaluate the selectivity of the proposed method, the fluorescence responses of the sensing system to M.SssI MTase and bovine serum albumin (BSA) were tested and compared with that to Dam MTase. M.SssI

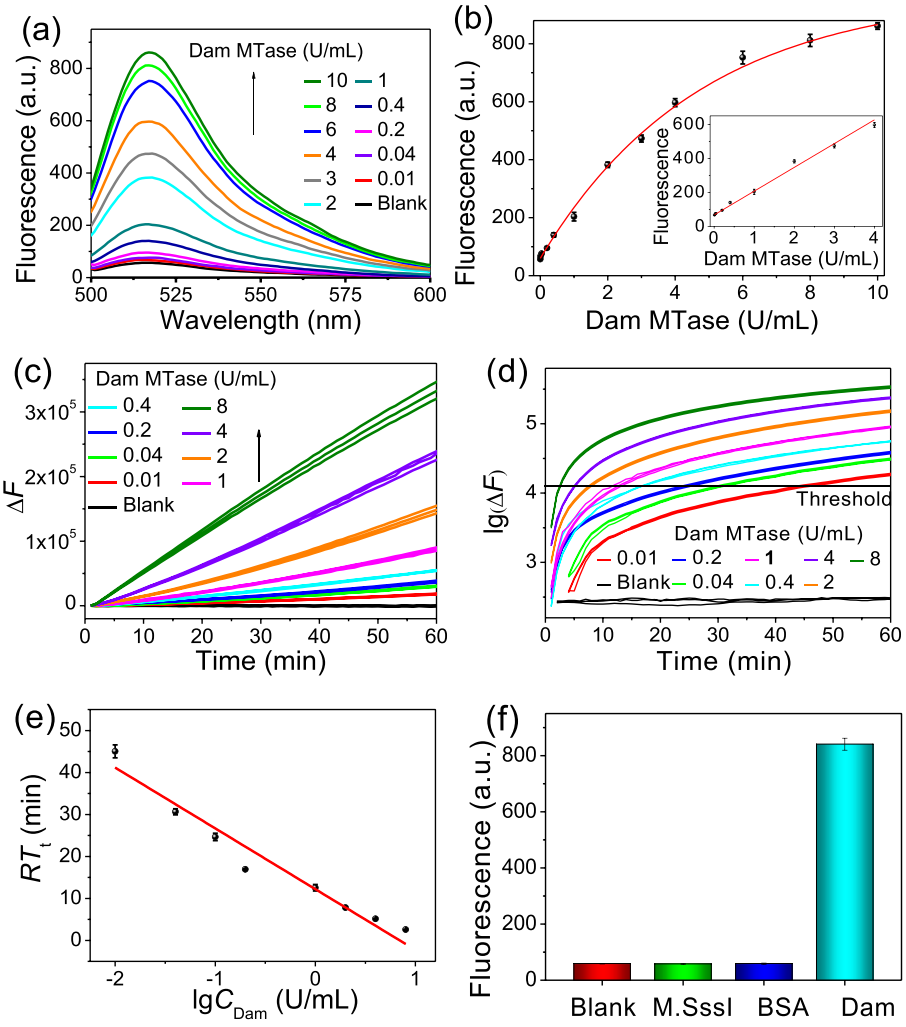


**Fig. 2.** Sensitivity and selectivity of the Dam MTase-sensing system. (a) Fluorescence spectra of the sensing systems containing different concentrations of Dam MTase. (b) Dam MTase concentration-dependent change in the fluorescence intensity at 517 nm. The insert shows the linear relationship between the fluorescence intensity and the Dam MTase concentration in the range of 0.01–4 U/mL. (c) $\Delta F \sim$ time curves obtained in real-time detection mode. (d) $\lg(\Delta F) \sim$ time curves derived from the $\Delta F \sim$ time curves. (e) The linear correlation between the $RT_t$ value and the logarithm of Dam MTase concentration. (f) Fluorescence responses of the sensing system to 8 U/mL Dam MTase, 8 U/mL M.SssI MTase and 200 μg/mL BSA. Error bars represent the standard deviation of three independent experiments.

MTase is also a member of methyltransferase family. Different from Dam MTase that methylates the adenine residue in 5′-GATC-3′, M.SssI MTase is responsible for methylation of the cytosine residue in 5′-CG-3'. As shown in Fig. 2f, significant fluorescence enhancement was observed in the presence of Dam MTase. In contrast, neither M.SssI MTase nor BSA could give detectable fluorescence change compared to the blank control, thus clearly demonstrating that our proposed method possesses excellent selectivity towards Dam MTase.

### 3.4. Dam MTase recovery in complex biological sample

As mentioned above, the unique working mechanism (TdT-catalyzed formation of intact Nt.BbvCI recognition site) can endow our method with improved anti-interference capability and thus increased application potential in real biological samples. To validate the practical application feasibility of the proposed sensing system, three different concentrations of Dam MTase (0.200, 1.000 and 4.000 U/mL) were added in healthy human serum samples and the recovery rates were tested. The results are given in Table 2. The recoveries of the method were found to be in the range of 98.72–105.1%. The results showed that this method has great potential for the accurate detection of MTase in complex biological samples.

**Table 2**
Recovery of Dam MTase tested in human serum sample.

| Spiked Dam (U/mL) | Detected Dam (U/mL) | Recovery (%) n = 3 |
|---|---|---|
| 0.200 | 0.1977 ± 0.0208 | 98.85 ± 1.04 |
| 1.000 | 0.9872 ± 0.0160 | 98.72 ± 1.60 |
| 4.000 | 4.203 ± 0.040 | 105.1 ± 1.0 |

### 3.5. Dam MTase activity inhibition assay

Since MTase is associated with the virulence of bacterial pathogens, the screening of MTase inhibitors can provide an effective tool for antibacterial therapeutic applications. In this research, 5-fluorouracil was selected as the model inhibitor to investigate the feasibility of the proposed method for the screening of MTase-targeted antimicrobial drugs. Considering the involvement of Dpn I, TdT and Nt.BbvCI in this sensing platform, it is essential to preclude the possibility that the inhibitor has influence on these enzymes. Therefore, two experiments were designed. In the first experiment, 5-fluorouracil was added after treatment of $\mathbf{eS_{Dam}}$ with Dam MTase and Dpn I. The results showed that the fluorescence intensity of the sensing system had no obvious difference from that obtained in the absence of 5-fluorouracil (Fig. S9a), thus indicating that 5-fluorouracil has no obvious effect on the activities of TdT and Nt.BbvCI. In the second experiment, $\mathbf{eS_{Dam}}$ was firstly treated with Dam MTase. Then, 5-fluorouracil and Dpn I (or Dpn I alone) were added. And again, the sensing systems with or without 5-fluorouracil gave comparable fluorescence outputs (Fig. S9b), thus suggesting that 5-fluorouracil also has no detectable effect on Dpn I activity. After precluding the effects on other enzymes, the inhibition capability of 5-fluorouracil towards Dam MTase was tested. According to the dose-dependent relationship between fluorescence signal output

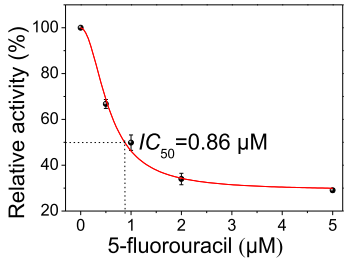


**Fig. 3.** Relative activity of 0.4 U/mL Dam MTase in the presence of increasing concentrations of 5-fluorouracil.

and 5-fluorouracil concentration (Fig. 3), an $IC_{50}$ value (the 5-fluorouracil concentration resulting in 50% inhibition of Dam MTase activity) was calculated to be 0.86 μM, which is consistent with that reported in the literature[40]. This result indicates that the proposed method could be applied to screen MTase inhibitors and evaluate their inhibitory capabilities.

### 3.6. TdT-NEAR-based T4 PNK-sensing assay

To demonstrate the generality of our proposed isothermal signal amplification strategy, we established another sensing platform for analysis of T4 PNK activity. The working principle of the proposed T4 PNK platform is shown in Fig. 4a. To achieve the detection of T4 PNK activity, the same fluorescent probe **F-Q** is used and the enclosed dumbbell-shaped substrate is replaced by a much simpler linear substrate $\mathbf{S_{PNK}}$. $\mathbf{S_{PNK}}$ contains an incomplete Nt.BbvCI recognition sequence (5′-GCTGA-3′) at the 3′-end. Due to the presence of 3′-end phosphorylation modification, $\mathbf{S_{PNK}}$ cannot be extended by TdT. Upon treatment with PNK, however, the 3′-phosphate group of this substrate is converted into 3′-OH. Then, TdT-activated Nt.BbvCI-catalyzed cyclic signal amplification can be initiated. Fluorescence analysis confirmed the feasibility of the designed platform (Fig. 4b). That is, only the sensing system containing $\mathbf{S_{PNK}}$, **F-Q**, T4 PNK, TdT and Nt.BbvCI displayed significantly increased fluorescence. On the contrary, the fluorescence of the negative controls lacking T4 PNK, TdT or Nt.BbvCI barely changed. Fig. 4c showed that the fluorescence intensity is linearly proportional to PNK activity in the range of 0.001–0.05 U/mL with a detection limit of $4 \times 10^{-4}$ U/mL, which is comparable or better than those reported by others (Table S2) (Cui et al., 2018; Feng et al., 2018; Liu et al., 2018; Gao et al., 2017). The sensing platform can also be used for T4 PNK inhibitor screening and inhibitor activity evaluation. The $IC_{50}$ value of $(NH_4)_2SO_4$, a well-known T4 PNK inhibitor, was calculated to be 12.42 mM (Fig. 4d), approximate to the reported value in previous studies (Li et al., 2017, 2018b). Moreover, this sensor was also demonstrated to work well for the detection of PNK activity in cell lysates. As shown in Fig. 4e and f, significant fluorescence enhancement could be observed with the addition of the lysates of HeLa (human

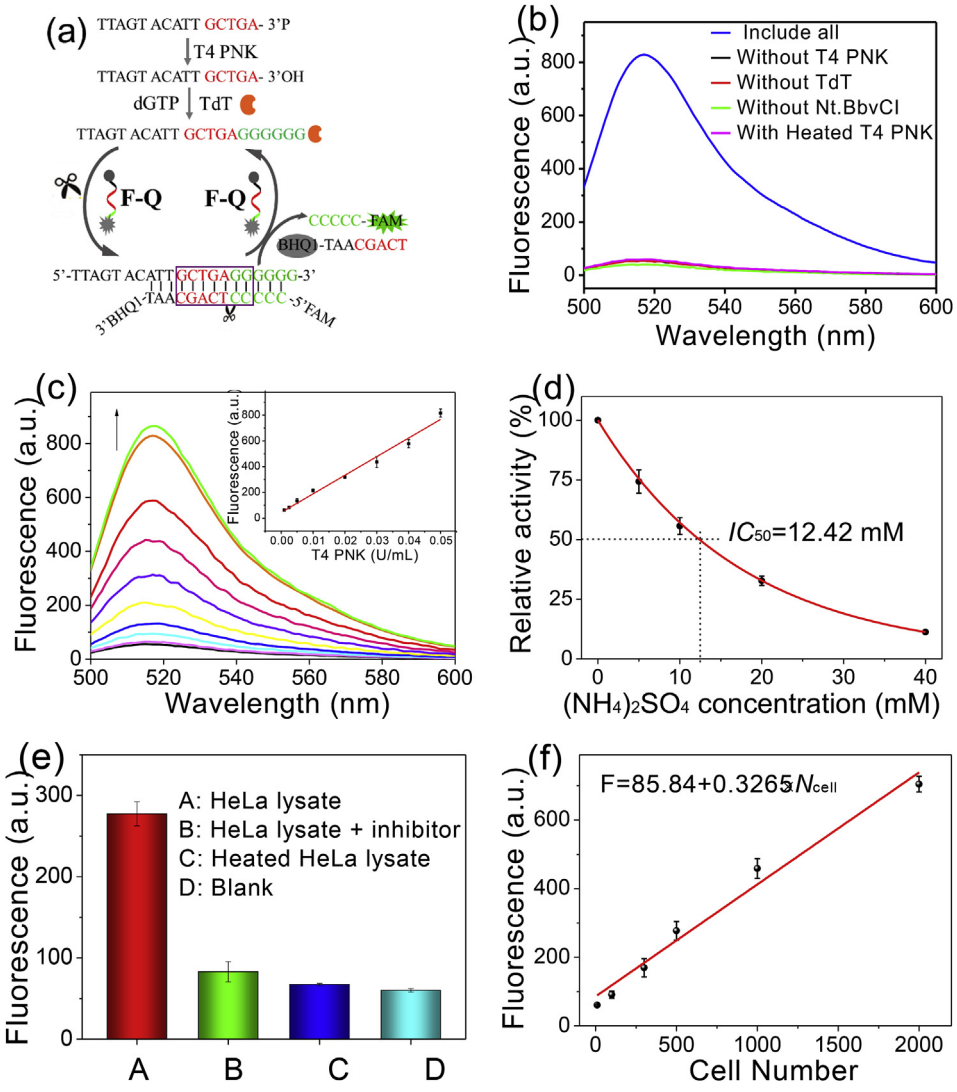


**Fig. 4.** (a) Schematic illustration of TdT-NEAR-based T4 PNK activity assay. (b) Fluorescence assay for different sensing systems. [T4 PNK] = 0.05 U/mL. (c) T4 PNK concentration-dependent change in the fluorescence at 517 nm. The T4 PNK concentration are (arrow direction): 0, 0.001, 0.0025, 0.005, 0.01, 0.02, 0.03, 0.04, 0.05 and 0.1 U/mL, respectively. Insert indicates the linear relationship between the fluorescence intensity and the T4 PNK concentration in the range of 0.001–0.05 U/mL. (d) Inhibition of PNK activity by $(NH_4)_2SO_4$. [PNK] = 0.01 U/mL. (e) Fluorescence intensities of different sensing systems. Lysates are extracted from 500 HeLa cells. $[(NH_4)_2SO_4]$ = 40 mM. (f) PNK activity detection in cell lysates. Linear relationship between fluorescence intensity and the HeLa cell number in the range of 10–2000 HeLa cells was obtained.

cervical cancer cell line) cells. It is worth noting that, after preincubated with inhibitor or heated at 95 °C for 10 min, the cell lysates could only cause slight fluorescence changes compared to the blank control, thus demonstrating that the fluorescence enhancement caused by cell lysates is indeed related with active PNK. Then, endogenous PNK activity in HeLa cell lysates was quantified, and it was estimated to be about $2.3 \times 10^{-4}$ U per cell, which is consistent with reported results (Li et al., 2018b). Collectively, these results indicated that the proposed TdT-NEAR strategy has wide application potential in analysis of some important enzymes. In the **F-Q** probe used in this work, the fluorophore and the quencher are labelled at the two ends. To further decrease the background fluorescence of the sensing systems, a feasible way is to shorten the distance between the fluorophore and the quencher in the probe. That is, the fluorophore and the quencher are labelled at two adjacent nucleotides that locate at the two sides of the nicking site. However, the probe synthesis cost will inevitably increase.

## 4. Conclusion

In conclusion, we have developed a TdT-NEAR strategy for the sensitive and specific detection of Dam MTase and T4 PNK activity. The high signal amplification efficiency endows the sensing platforms with high sensitivities and low detection limits of 0.002 U/mL for Dam MTase and $4 \times 10^{-4}$ U/mL for T4 PNK, respectively. The unique working mechanism involving TdT-induced formation of intact Nt.BbvCI recognition site overcomes the inherent drawback of TdT-based biosensors, thus giving the proposed methods with greatly increased potential for applications in complex biological samples, including human serum and cancer cells. What's more, the sensing platforms were also demonstrated to work well for screening MTase or PNK inhibitors and evaluating their inhibitory capacities. This work may provide a new paradigm for nucleic acid-based signal amplification and may find wide applications in biomedical research and clinical diagnosis.

## CRediT authorship contribution statement

**Yi-Chen Du:** Funding acquisition, Methodology, Conceptualization, Investigation, Writing - original draft, Data curation. **Si-Yuan Wang:** Data curation, Investigation. **Xiao-Yu Li:** Investigation. **Ya-Xin Wang:** Formal analysis. **An-Na Tang:** Supervision. **De-Ming Kong:** Funding acquisition, Resources, Writing - review & editing, Supervision.

## Declaration of competing interest

The authors declare that they have no known competing financial interests or personal relationships that could have appeared to influence the work reported in this paper.

## Acknowledgment

This work was supported by the National Natural Science Foundation of China (Nos. 21874075, 21728801) and the Fundamental Research Funds for Central Universities, Nankai University (Nos. 63191523, 63191728,63191310).

## Appendix A. Supplementary data

Supplementary data to this article can be found online at https://doi.org/10.1016/j.bios.2019.111700.

## References

Bernstein, N.K., Williams, R.S., Rakovszky, M.L., Cui, D., Green, R., Karimi-Busheri, F., Mani, R.S., Galicia, S., Koch, C.A., Cass, C.E., Durocher, D., Weinfeld, M., Glover, J.N.M., 2005. Mol. Cell 17, 657–670.
Boye, E., Marinus, M.G., Lobner-Olesen, A.J., 1992. Bacteriol 174, 1682–1685.
Chappell, C., Hanakahi, L.A., Karimi-Busheri, F., Weinfeld, M., West, S.C., 2002. EMBO J. 21, 2827–2832.
Chen, R., Shi, H., Meng, X., Su, Y., Wang, H., He, Y., 2019a. Anal. Chem. 91, 3597–3603.
Chen, Y., Meng, X.-Z., Gu, H.-W., Yi, H.-C., Sun, W.-Y., 2019b. Biosens. Bioelectron. 134, 117–122.
Cheng, R., Tao, M., Shi, Z., Zhang, X., Jin, Y., Li, B., 2015. Biosens. Bioelectron. 73, 138–145.
Cheng, X., Roberts, R.J., 2001. Nucleic Acids Res. 29, 3784–3795.
Cui, L., Li, Y., Lu, M., Tang, B., Zhang, C.-Y., 2018a. Biosens. Bioelectron. 99, 1–7.
Cui, L., Hu, J., Li, C.-C., Wang, C.-M., Zhang, C.-Y., 2018b. Biosens. Bioelectron. 122, 168–174.
Cui, Y.X., Feng, X.N., Wang, Y.X., Pan, H.Y., Pan, H., Kong, D.M., 2019. Chem. Sci. 10, 2290–2297.
Deng, S., Yan, J., Wang, F., Su, Y., Zhang, X., Li, Q., Liu, G., Fan, C., Pei, H., Wan, Y., 2019. Biosens. Bioelectron. 137, 263–270.
Du, Y.C., Cui, Y.X., Li, X.Y., Sun, G.Y., Zhang, Y.P., Tang, A.N., Kim, K., Kong, D.M., 2018a. Anal. Chem. 90, 8629–8634.
Du, Y.C., Zhu, Y.J., Li, X.Y., Kong, D.M., 2018b. Chem. Commun. 54, 682–685.
Faber, J., Kantarjian, H., Roberts, M.W., Keating, M., Freireich, E., Albitar, M., 2000. Arch. Pathol. Lab Med. 124, 92–97.
Feng, C., Wang, Z., Chen, T., Chen, X., Mao, D., Zhao, J., Li, G., 2018. Anal. Chem. 90, 2810–2815.
Gao, M., Guo, J., Song, Y., Zhu, Z., Yang, C., 2017. ACS Appl. Mater. Interfaces 9, 38356–38363.
He, H.-Z., Leung, K.-H., Wang, W., Chan, D.S.-H., Leung, C.-H., Ma, D.-L., 2014. Chem. Commun. 50, 5313–5315.
Hou, T., Wang, X., Liu, X., Lu, T., Liu, S., Li, F., 2014. Anal. Chem. 86, 884–890.
Hou, T., Xu, N., Wang, W., Ge, L., Li, F., 2019. Biosens. Bioelectron. 141, 111395.
Huang, J., Li, X.Y., Du, Y.C., Zhang, L.N., Liu, K.K., Zhu, L.N., Kong, D.M., 2017. Biosens. Bioelectron. 91, 417–423.
Ji, J., Liu, Y., Wei, W., Zhang, Y., Liu, S., 2016. Biosens. Bioelectron. 85, 25–31.
Jiang, H.-X., Kong, D.-M., Shen, H.-X., 2014. Biosens. Bioelectron. 55, 133–138.
Kim, B.Y., Kwon, O.S., Joo, S.A., Park, J.A., Heo, K.Y., Kim, M.S., Ahn, J.S., 2004. Anal. Biochem. 326, 21–24.
Lindahl, T., Wood, R., 1999. Science 286, 1897–1905.
Li, C., Wang, H., Shang, J., Liu, X., Yuan, B., Wang, F., 2018a. ACS Sens. 3, 2359–2366.
Li, J., Yan, H., Wang, K., Tan, W., Zhou, X., 2007. Anal. Chem. 79, 1050–1056.
Li, X., Xu, X., Song, J., Xue, Q., Li, C., Jiang, W., 2017. Biosens. Bioelectron. 91, 631–636.
Li, X.-Y., Du, Y.-C., Pan, Y.-N., Su, L.-L., Shi, S., Wang, S.-Y., Tang, A.-N., Kim, K., Kong, D.-M., 2018b. Chem. Commun. 54, 13841–13844.
Lin, L., Liu, Y., Zhao, X., Li, J., 2011. Anal. Chem. 83, 8396–8402.
Liu, M., Ma, F., Zhang, Q., Zhang, C.Y., 2018. Chem. Commun. 54, 1583–1586.
Liu, Z., Li, W., Nie, Z., Peng, F., Huang, Y., Yao, S., 2014. Chem. Commun. 50, 6875–6878.
Ma, F., Liu, W.J., Tang, B., Zhang, C.Y., 2017. Chem. Commun. 53, 6868–6871.
Peng, Y., Jiang, J., Yu, R., 2013. RSC Adv. 3, 18128–18133.
Rajendran, G., Shanmuganandam, K., Bendre, A., Muzumdar, D., Goel, A., Shiras, A.J., 2011. Neuro Oncol. 104, 483–494.
Rauf, S., Zhang, L., Ali, A., Ahmad, J., Liu, Y., Li, J., 2017. Anal. Chem. 89, 13252–13260.
Rebeck, G.W., Samson, L.J., 1991. Bacteriol 173, 2068–2076.
Reik, W., Dean, W., Walter, J., 2001. Science 293, 1089–1093.
Robertson, K.D., Uzvolgyi, E., Liang, G., Talmadge, C., Sumegi, J., Gonzales, F.A., Jones, P.A., 1999. Nucleic Acids Res. 27, 2291–2298.
Roll, J.D., Rivenbark, A.G., Jones, W.D., Coleman, W.B., 2008. Mol. Cancer 7, 15.
Sharma, S., Doherty, K., Brosh, R., 2006. Biochem. J. 398, 319–337.
Shukla, V., Coumoul, X., Lahusen, T., Wang, R.H., Xu, X., Vassilopoulos, A., Xiao, C., Lee, M.H., Man, Y.G., Ouchi, M., Ouchi, T., Deng, C.X., 2010. Cell Res. 20, 1201–1215.
Smith, Z.D., Meissner, A., 2013. Nat. Rev. Genet. 14, 204–220.
Wang, L.J., Han, X., Li, C.C., Zhang, C.Y., 2018. Chem. Sci. 9, 6053–6061.
Wang, Q., Pan, M., Wei, J., Liu, X., Wang, F., 2017. ACS Sens. 2, 932–939.
Wang, Y., He, X., Wang, K., Su, J., Chen, Z., Yan, G., Du, Y., 2013. Biosens. Bioelectron. 41, 238–243.
Wenzel, C., Guschlbauer, W., 1993. Nucleic Acids Res. 21, 4604–4609.
Wu, Z., Wu, Z.K., Tang, H., Tang, L.J., Jiang, J.H., 2013. Anal. Chem. 85, 4376–4383.
Xing, X.W., Tang, F., Wu, J., Chu, J.M., Feng, Y.Q., Zhou, X., Yuan, B.F., 2014. Anal. Chem. 86, 11269–11274.
Xu, X., Wang, L., Cui, W., Jiang, W., 2018. Sens. Actuators B Chem. 266, 124–130.
Yuan, Y., Li, W., Liu, Z., Nie, Z., Huang, Y., Yao, S., 2014. Biosens. Bioelectron. 61, 321–327.
Zeng, Y.P., Hu, J., Long, Y., Zhang, C.Y., 2013. Anal. Chem. 85, 6143–6150.
Zhang, Y., Wang, X.Y., Zhang, Q., Zhang, C.Y., 2017. Anal. Chem. 89, 12408–12415.
Zhang, Y., Xu, W., Zeng, Y., Zhang, C.Y., 2015. Chem. Commun. 51, 13968–13971.
Zhou, Y., Fang, W., Lai, K., Zhu, Y., Bian, X., Shen, J., Li, Q., Wang, L., Zhang, W., Yan, J., 2019. Biosens. Bioelectron. 141, 111419.
Zhu, L., Chen, D., Lu, X., Qi, Y., He, P., Liu, C., Li, Z., 2018. Chem. Sci. 9, 6605–6613.